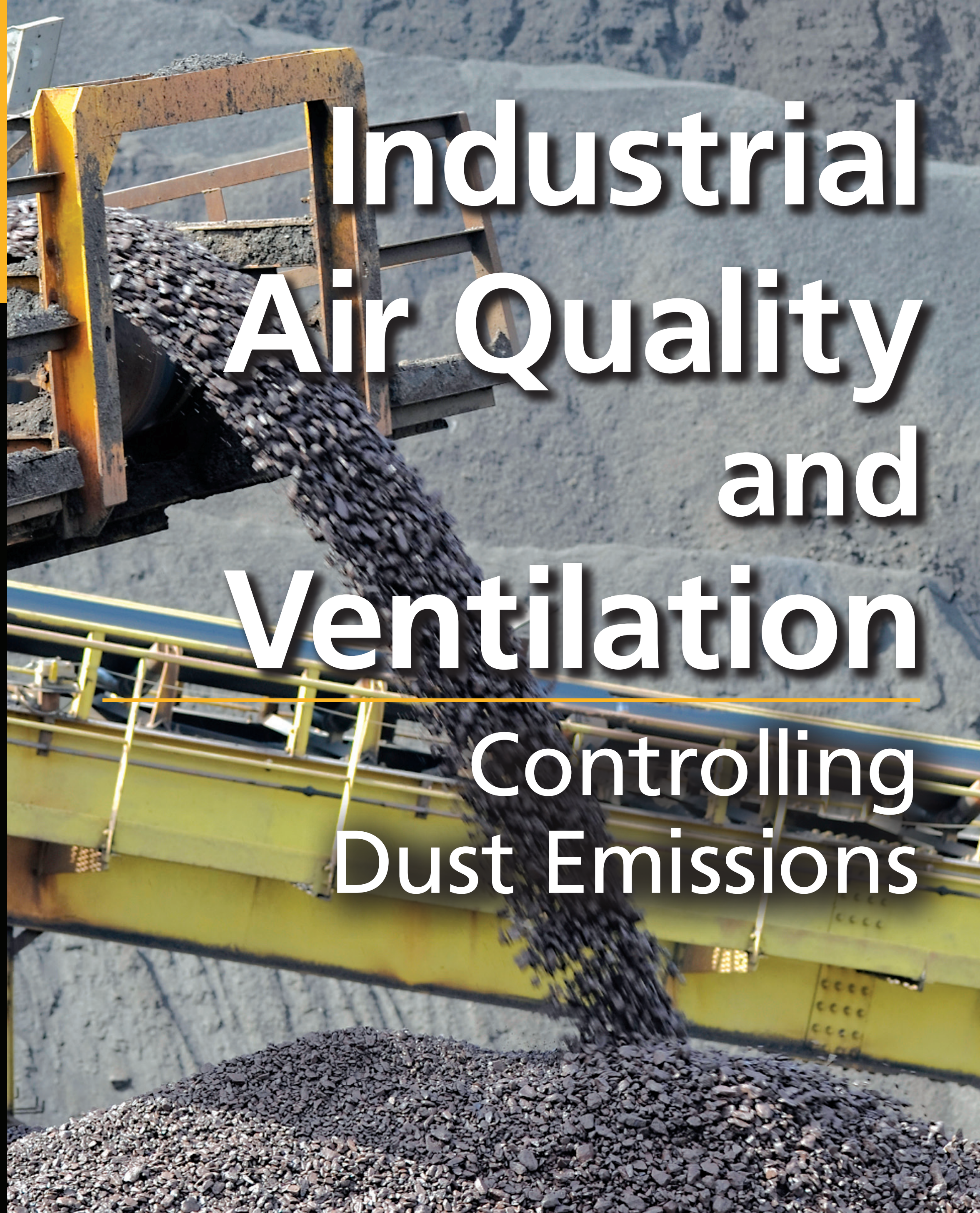

Industrial Air Quality and Ventilation

Controlling Dust Emissions

Ivan Nikolayevich Logachev
Konstantin Ivanovich Logachev

CRC Press
Taylor & Francis Group

Industrial Air Quality and Ventilation

Controlling Dust Emissions

Industrial Air Quality and Ventilation

Controlling Dust Emissions

Ivan Nikolayevich Logachev
Konstantin Ivanovich Logachev

CRC Press
Taylor & Francis Group
Boca Raton London New York

CRC Press is an imprint of the
Taylor & Francis Group, an **informa** business

CRC Press
Taylor & Francis Group
6000 Broken Sound Parkway NW, Suite 300
Boca Raton, FL 33487-2742

Version Date: 20130923

International Standard Book Number-13: 978-1-4822-2217-3 (eBook - PDF)

Visit the Taylor & Francis Web site at
http://www.taylorandfrancis.com

and the CRC Press Web site at
http://www.crcpress.com

Contents

Preface

There has always been interest in the most precise answer to the question of suction hood capacity. The lack of an in-depth analysis of aerodynamic processes and properly equipped computer facilities has meant that specialists had to be content with the simplest proportions. Typically used was an empirical approach based on crude models (if not on one's intuition) or on such vague notions as "practical data" or "countertypes." Therefore, an answer was quite often approximate: dust exhaustive plant capacity was either assumed to be within a great margin, which contributed to lower service quality and higher power consumption, or was much lower than the required values, which decreased the sanitary and hygienic effect.

This volume is devoted to studying air injection into granular material streams and to defining the closed hood capacity widely used in mechanical reprocessing of minerals. An air injection mechanism used with a solid stream has been discovered for two typical cases of bulk material flow: when transferring in closed chutes and in gravity bulking, which allowed for detailing accurate methods of aspiration volume calculation for transfer groups featuring diverse chute configurations in view of the aerodynamic connections of extract hoods.

The authors did not integrate published study findings for this subject but took a chance on familiarizing the reader primarily with findings from their own studies conducted during several years of work in the All-Union Research and Development Institute of Occupational Safety in Metal Mining Industry (VNIIBTG, Krivoy Rog) and in the Belgorod Shukhov State Technology University (BSTU), from which the members' support, assistance, and positive help are sincerely appreciated.

We also credit our teachers V. V. Nedin, O. D. Neikov, and A. V. Sheleketin, and our colleagues V. A. Minko, R. N. Shumilov, A. M. Golyshev, S. I. Zadorozhny, V. V. Kachanov, V. I. Stukanova, L. M. Chernenko, and all workers at the VNIIBTG Industrial Ventilation Laboratory and at the BSTU Department of Heat, Gas Supply, and Ventilation, whose attention and direct cooperation, creative debates, and discussions of findings enabled the authors to practically demonstrate their ideas.

The reported study was partially supported by the Council for Grants of the President of the Russian Federation (projects NSH-588.2012.8), RFBR (project number 12-08-97500-p_center_a) and Strategic Development Program of Belgorod State Technological University named after V. G. Shukhov (project number A-10/12).

Symbols

a_T	acceleration of a stream of particles in a chute, m^2/s
$B(b)$	half-width of a plane jet of particles, m
c	airborne speed of particles, m/s
c_y	conventional airborne speed, m/s
c_1	heat capacity of material particles, J/(kg·K)
c_2	air heat capacity (with p = const), J/(kg·K)
D	hydraulic diameter of a chute (channel), m
d, d_E, d_e	particle diameter (sphere diameter equivalent to a particle in terms of volume), m
E	specific energy, J/kg
e	specific enthalpy, J/kg
F_{21}	interacting force between air and stream volume unit particles, N/m^3
F	leakage area (F_b, upper hood; F_H, lower hood), m^2
f_M, f_P	particle frontal area, m^2
G	mass flow (G_1, particles; G_2, air; G_B, dry air), kg/s
g	gravity factor (g_x, chute x-direction gravity factor), m/s^2
H	drop height of particles, m
$h = x = x/l_\infty$	dimensionless drop height of particles
I	intensity of interphase transformations, $kg/(s \cdot m^3)$
k	particle drag coefficient (k_g, k_f, k_s, geometric; k_∂, dynamic)
k_m	particle frontal area/volume ratio, 1/m
L_E, Q_E	induced airflow in a chute, m^3/s
l	chute length, m
l_∞	characteristic length (inertial course length), m
M	mass force (M_1, particles; M_2, air), N/kg
m, m_P	particle mass, kg
n_P, n_1	particle count, $1/m^3$
n	relation of the initial particle speed in a chute to the particle speed in the chute channel
P	pressure (p_E, p_e chute injection pressure; P_T, chute thermal pressure; P_α, P_0, outside chute; P_j, chute interphase pressure), Pa
$\mathbf{P} = P / (\rho_2 c^2)$	dimensionless pressure
P_p	particle weight, N

Q_{ch}	chute airflow, m^3/s
Q_{21}	air-to-particles heat exchange rate, W/m^3
q	heat flow, W/m^2
R	aerodynamic drag of bombarding particles, N
R_{21}	air impact on solid particle, N
P_{Π}	aerodynamic force of stream particle, N
R, R_0	aerodynamic force of single particle, N
R_{ch}	chute hydraulic characteristic, kg/m^7; $Pa/(m^3/s)^2$
S	area of particles flow section, m^2
S, S_{ch}	cross sectional area of a chute (channel), m^2
s	surface (s_P, particles; s_L, sphere), m^2
T	temperature,°K
T_{2mean}	mean air temperature in a chute, °K
T_0	average air temperature outside a chute, °K
t, τ	time (τ_∞, relaxation time), s
V	volume (V_P, particle volume), m^3
υ, v, □	velocity (υ, υ_1, particles; υ_{1k}, υ_k, particles at the chute outlet; υ_{10}, υ_{1H}, particles at the chute inlet; υ_2, u, air), m/s
u_{BX}	exhaust pipe entry section air velocity, m/s
$w = \upsilon - u$	relative particle velocity, m/s
w	material humidity,%
x	path of particles over a chute, m
α	interelement exchange ratio (α_m, mass, $kg/(s\cdot m^2\cdot K)$; α_T, α, heat, $W/(m^2\cdot K)$)
β	volume concentration (β_1, particles; β_2, air), m^3/m^3
β_T	air thermal expansion coefficient, 1/°K
ε	air-to-particles density ratio
ζ	local drag factor (LDF)
η, μ	absolute viscosity coefficient, Pa·s
θ	horizontal chute angle
λ	hydraulic resistance coefficient
λ_g	air thermal conductivity, W/(m·K)
ν	air kinematic viscosity coefficient, m^2/s
$\vec{\Pi}$	surface force vector, N/m^2
Π_C	material particle constraint ratio, without unit of measurement
Π_d	dynamical interference activity factor, without unit of measurement

ρ	density (ρ_1, ρ_m, particle material; ρ_2, ρ, particle stream air; ρ_0, air outside a chute; ρ_{2H}, ρ_{2K}, air at the chute inlet and outlet), kg/m^3
τ	time, s
τ	tangential stress, Pa
φ, φ_k	component slip ratio (relation of the induced air speed to the particle speed at the chute outlet), without unit of measurement
ψ	particle resistance coefficient ($\psi_{0,}$ particles in the area of self-similarity; ψ_{0L}, sphere in the area of self-similarity; $\psi_{c,}$ airborne particles; ψ^*, stream particles), without unit of measurement

CRITERIA

$Re = wd\rho/\eta$	Reynolds number
$Fr = gh / \upsilon_1^2$	Froude number
$Fr^* = G_1 g / \left(\upsilon_1^3 b \rho_1\right)$	modified Froude number
$Bu = \psi^* k_m G_1 \upsilon_{1k} / \left(\sum \zeta a_T S_{ch} \rho_1\right)$	Butakov–Neikov number
$Eu = S_{ch} \dfrac{c_y}{2} \rho_0 / (G_1 v_{1k}), Eu^* = \Delta p / \left(0{,}5 \sum \zeta \upsilon_{1k}^2 \rho_2\right)$	Euler number
$Gr = \beta_T \dfrac{gH^3}{\nu^2} (T_{2av} - T_0)$	Grashof number
$Nu = \alpha d / \lambda_g$	Nusselt number

1 Dust and Air Mechanics of Bulk Material Transfer

Bulk material transfer (gravity transportation by chutes) is the most widespread operation for reprocessing mineral raw materials: mining and beneficiation of ore and coal, sintering of concentrates, stock preparation in ferrous and nonferrous metallurgy, and production of building materials. Bulk material flow results in considerable dust emission. With the great volume of mineral raw materials that are reprocessed, such dust emissions significantly impact the overall balance of airborne atmospheric pollution. Dust emissions are dangerous not only from the standpoint of toxicity and occupational disease but also because of the negative impact on the environment.

Ore preparation plants that serve major iron ore deposits are primary sources of dust emissions in terms of capacity and diversity. Highly intensive bulk material transfer operations at plants such as the Northern, Novo-Krivorozhskiy, Southern, and Inguletskiy mining and concentration complexes of Krivbass; the Lebedinskiy, Mikhailovskiy, and Stoylenskiy mining and concentration complexes of the Kursk Magnetic Anomaly (KMA) basin; the Kostomukshskiy, Olenegorskiy, and Kovdorskiy mining and concentration complexes of the southwestern district of Russia; and the Kachkanarskiy (Ural) and Sokolovsko-Sarbayskiy (Kazakhstan) mining and concentration complexes feature any number of dust-producing sources: crushed ore, iron ore concentrate, agglomerate, pellets, bentonite, limestone, and charred coal. The most environmentally unfriendly are agglomerate and pellets generated from sintering of fine-grained concentrate. Transferring such materials produces a major dust release (e.g., when loading and unloading rail cars or stacking unused materials in storage).

The main cause of dust discharge is ejection, that is, directional air flow formation within a stream of a bulk material resulting from interaction between bombarding particles and air. Studying regularities in induced air flow occurrence enables forecasting air pollution levels and aerosol emission, thereby making it possible to select the optimum engineering solutions for air containment and dedusting. This can be demonstrated using bulk material transfer technology in ore preparation plants as an example, including the diversity of materials, the material handling processes, and the process equipment.

1.1 TRANSFER GROUPS AS AIR POLLUTION SOURCES

1.1.1 Intensity of Dust Emissions

In terms of atmospheric pollution, dust transfer groups are conventionally divided into external and internal types. The dust emissions from outdoor (external) transfer groups pollute the ground level air of mine sites. Internal transfer groups are located in production areas and pollute the intrashop air. The dust generation mechanism is the same for both and differs only in dust cloud propagation. Although dust particles in a shop are transported exclusively by means of diffusion and convective air flows when transferring hot materials, the outdoor process is supplemented by wind force.

An immediate dusting of the ground level air occurs:

- When conveying, grating, or breaking the ore mass (typical of the cyclical and continuous method of ore delivery in open-cut mines)
- When feeding receiving funnels of dressing plant primary crushers
- When discharging agglomerate raw materials from indurating and sintering machines
- When loading rail cars with agglomerate and burnt pellets
- With outdoor storage and the blending of bulk mining materials
- With open-cut mines
- In mining and concentration complex plants

The intensity of dust emissions depends on the type of process operations and the physical and mechanical properties of the reprocessed material as well as the availability of dust control arrangements (Table 1.1).

The transfer of agglomerate and pellets results in the highest dust emission intensity. This can be demonstrated by analyzing the specific gross dust emissions by iron ore integrated works and by reprocessing operations in general (Figure 1.1). Gross dust emissions from all transfer groups at sintering plants (such as the sintering plants of YuGOK and NKGOK and the pellet plants of SevGOK) are greater than dust emissions at crushing and dressing plants (InGOK). This excess is noticeable in specific dust emissions in terms of mass (q, kg per ton of reprocessed material) and volume (Q, thous. m^3/t; i.e., aspirated dusty air volume per ton of reprocessed material). Sintering and pelletizing processes are much "dustier" than dressing and crushing processes. This is also noticeable when feeding conveyers (Figure 1.2): due to high strength and apparent humidity, natural minerals (e.g., iron ore) feature much poorer dust-making properties than artificial materials resulting from thermal treatment (agglomerate, pellets). The greatest amount of dust-making results from loading agglomerate and pellets in rail cars (hopper cars, pellet cars, dump cars) and from stocking operations (Figure 1.3).

Dust generation, when transferring bulk materials, is mainly caused by dust fractions that have been suspended for a time. Dust fractions result from mechanical reduction of minerals in crushers and mills, as well as from the impact of bombarding particles with each other and with chute walls.

Strong minerals are reprocessed in the metal mining industry; therefore, dust could be formed mainly out of fine fractions present in transferred materials. More fractions are found with artificial materials such as iron-ore pellets and agglomerate. Fraction content, in this case, is also determined by the quality of charging material and the evenness of its sintering in indurating machines. For instance, pellet firing in pipe furnaces (Poltavskiy mining and concentration

TABLE 1.1
Intensity of Bulk Material Transfer Dust Emissions

Equipment or Process Description	Intensity of Dust Emissions: Absolute, g/s	Intensity of Dust Emissions: Specific, g/t
1. Iron ore conveying in an open-cut mine		
(a) w/o dust control arrangements	0.4–3.0	3–22
(b) w/suction devices	0.03–0.3	0.02–2.2
2. Iron ore conveyer		
(a) w/o dust control arrangements	0.1–0.4	0.7–3
(b) w/iron ore sprinkling devices	0.05–0.2	0.3–1.5
3. Rumbling when screening ore at the CPT site		
(a) w/o means of containment	0.8–1.0	4–5
(b) w/ventilated hoods	0.07–0.09	0.3–0.5
4. Transferring iron ore from the conveyer to the CPT site storage stockpile		
(a) w/iron ore sprinkling	0.1–0.12	0.5–0.6
(b) w/containment of dust emissions	0.015–0.03	0.03–0.06
5. When breaking ore using self-propelled crushers		
SDA-300 (a) w/o means of containment	0.5–0.7	2.5–3.5
(b) w/suction devices	0.1–0.12	0.5–0.6
SDA-1000 (a) w/o means of containment	0.8–1.7	1.6–3.6
(b) w/suction devices	0.5–0.7	1.0–1.4
SDA-2000 (a) w/o means of containment	7–11	8–12
(b) w/suction and hydraulic dust control devices	1.8–2.3	2–2.5
6. Storing of chalky marl stones using ZP-5500 stocker		
(w/o dust control arrangements)	8–12	3–4
7. Transferring iron ore from a dump car into a short-shaft crusher receiving funnel		
(a) w/o dust control arrangements	16–30	1.6–3
(b) w/suction devices	2.5–5	0.3–0.5
8. Discharging agglomerate from sintering machine into a hopper		
(a) w/o ventilated tunnel	20	500
(b) w/suction devices	4	100
9. Discharging burnt pellets from bins into a hopper		
(a) w/o ventilated tunnel	15	300
(b) when loading via a telescopic chute	7	140
(c) w/ventilated tunnel	3	60
10. Transferring iron-ore pellets from UK-550 stacker to a stock pile		
(a) w/o dust control arrangements	15	30
(b) w/water sprinkling	8	16
(c) w/ventilated hoods	2	4

continued

TABLE 1.1 (Continued)
Intensity of Bulk Material Transfer Dust Emissions

Equipment or Process Description	Intensity of Dust Emissions Absolute, g/s	Intensity of Dust Emissions Specific, g/t
11. Transferring iron-ore pellets from a conveyer to UK-550 stacker beam conveyer		
(a) w/o dust control arrangements	3–7	6–14
(b) w/ventilated hoods	0.3–0.8	0.6–1.6
12. Transferring from 2R-550 rotary reclaimer wheel buckets when delivering pellets from a stock pile		
(a) w/o dust control arrangements	20	40
(b) w/hydraulic dust control devices	12	25

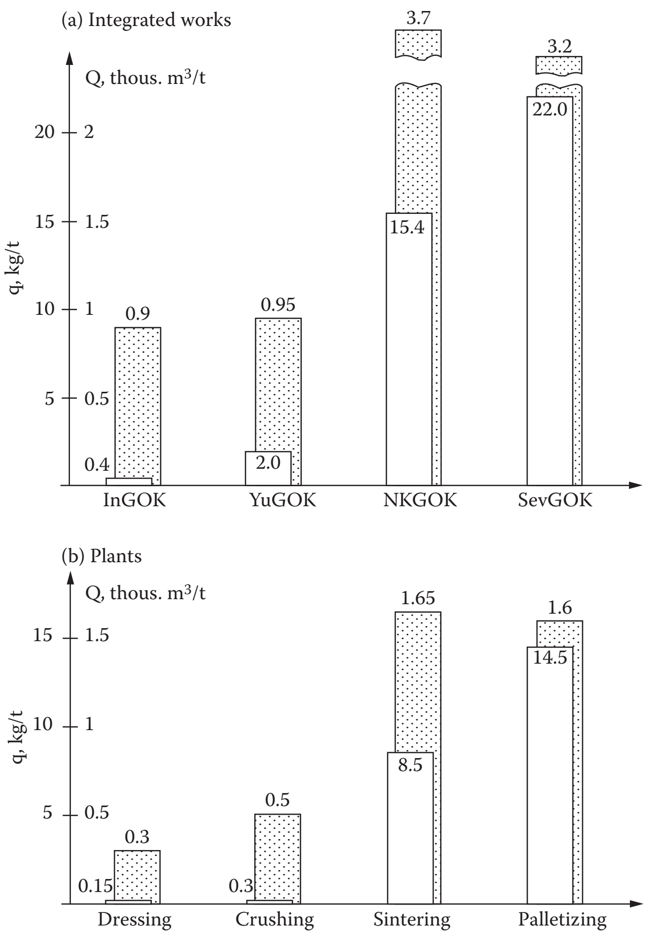

FIGURE 1.1 Specific dust emissions at Krivbass mining and concentration complexes.

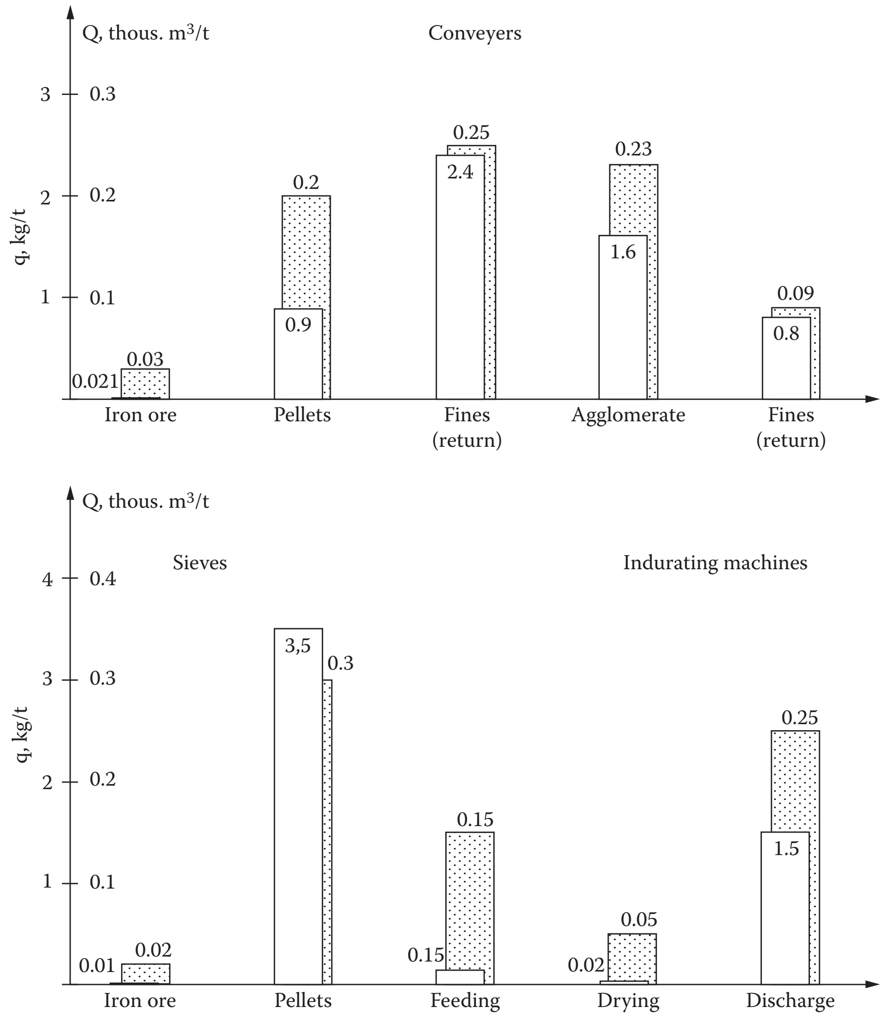

FIGURE 1.2 Specific dust emissions of ore preparation plants' processing equipment.

complex), where even heat treatment conditions are more favorable, yields stronger products with less dust content, especially compared to firing using conveyer-type machines.

The three successively alternating stages of dust emissions in bulk material transfer are:

- Free-falling material stream aeration
- Dynamic interaction of a particle stream bombarding at an increasing rate with air in transfer chutes
- Bleeding of induced dusty air from the stream when stacking particles on the conveyer belt

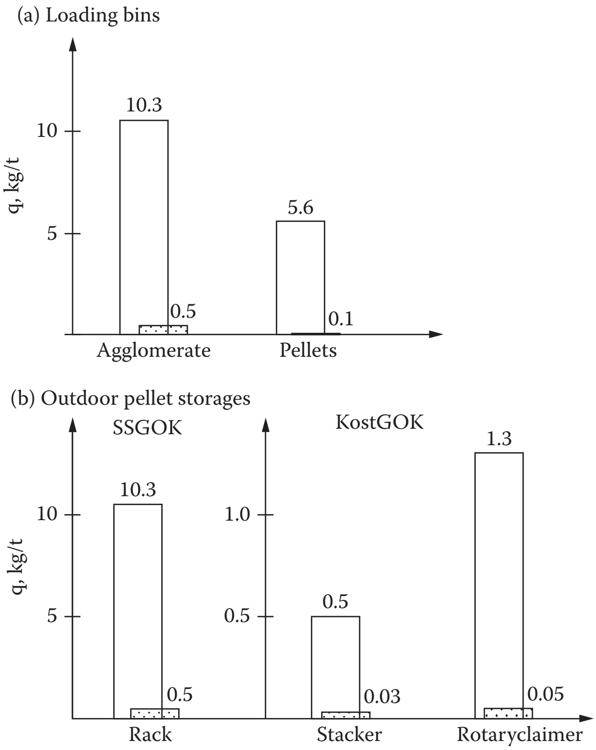

FIGURE 1.3 Specific dust emissions from land-based sources of iron ore sintering plants (the lower level results from the introduction of technical means described in Chapter 5).

The first stage features the interruption of self-adhesion forces between dust particles when discharging the material stream from the upper conveyer driving drum or feeder. An air dispersion system or dust aerosol begins to form. In free fall, the particle conglomerate discontinuity increases due to interaction with air and the collision with coarser particles and transfer chute walls. The induced air flow intensely fills with dust particles and forms an adhering jet of dusty air when bulk material is stacked on the lower conveyer.

Two facets of this stage are an inertial separation of particles and their sedimentation on the piled material surface and a blow-off of settled particles into the atmosphere. Therefore, the intensity of dust emissions is significantly influenced by the transferred material's humidity (which enhances the self-adhesion of fine particles) and by the material's pouring height (which determines the stream falling rate and the intensity of the dynamic interaction between particles and air).

Multiple experiments (see Chapter 5) showed that the primary factors determining the intensity of dust emissions are (Figure 1.4):

(a) Process parameters and physical and mechanical properties of bulk material:
  - Material humidity (W, %)

- Particle-size distribution—mean particle size (d_{mean}) and dust fraction weight content (a_d, %)
- Material flow rate (G_m, kg/s)
- Temperature (T_m,°K)
- Density of particles (ρ_m, kg/m^3)

(b) Design parameters of transfer chutes and hoods:

- Transfer height, or pouring height (H, m)
- Shape of chutes—inclination of straight portions of chutes ($\alpha_{i,}$ deg.), height of the same (H_i, m). and cross-sectional area (S_i, m^2)
- Hood type, which defines the optimum vacuum-gauge pressure (P_{opt}, Pa) and air injection resistance ($\Sigma\zeta$)
- Hood pressurization degree, which defines the leakage area (F_l, m^2)

Most of the parameters influence induced air volume, which defines dust discharge from hoods immediately in terms of lack of suction due to so-called unorganized sources of dust emissions and through suction volumes when such sources become unorganized. Air injection defines induced emission volume and has a significant effect on exhaust air dust concentration.

The quantitative interrelation among these parameters was first determined by V. A. Minko [61] and his students. He determined that the dust concentration depends on the weight content of dust fractions in the transferred material, a_d (particles finer than d_{max}, that is, the maximum diameter of dust particles blown out from

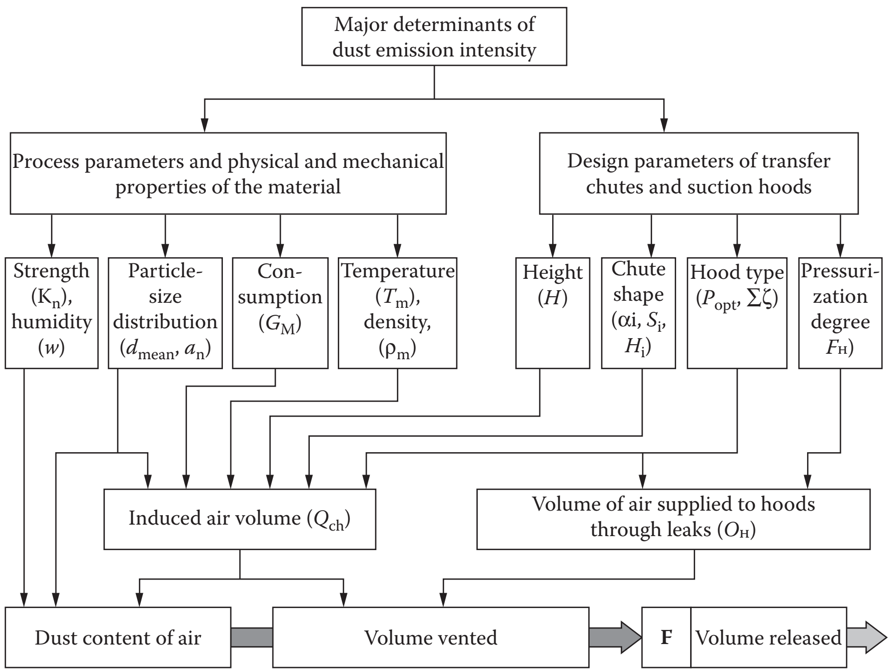

FIGURE 1.4 Major determinants of gross dust emissions in the transfer of bulk materials.

the hood). The maximum diameter value, in its turn, depends on the induced air flow, Q_{ch}, m^3/s; on the suction volume, Q_a, m^3/s; and on the geometric dimensions of the hood [204,205]:

$$d_{max} = 5780 \cdot \sqrt{\frac{Q_a}{\rho_M \cdot S_\Pi \cdot \left(1 + 0{,}08 \cdot \dfrac{Q_a \cdot S_{ch} \cdot L}{Q_{ch} \cdot S_\Pi \cdot H}\right)}},$$

where ρ_M is a density of particles, kg/m^3; S_{ch}, S_Π are cross-sectional areas of the chute and dust-collecting bag, m^2; H is the hood height, m; and L is the distance between the chute and the dust-collecting bag, m.

Dust discharge from a ventilated hood is similar to dust particle gravity sedimentation in a dust chamber: the bigger the hood and the lower the induced air volume, the lower the maximum size of particles blown out with the exhaust air, thereby resulting in lower dust content at the hood outlet.

1.1.2 Primary Means of Dust Emission Control

An analysis of current industrial ecology applications at ore preparation plants highlights three main trends for dust emission control in the transfer of bulk materials (Figure 1.5):

- Dust dilution in induced air [150,154,155,167,206]
- Reduction of air volume exhaust from ventilated hoods [130,150, 207,208]
- High-performance dedusting of suction emissions [123,164–166,209,210,211]

The most efficient method of dust dilution in induced air is watering materials (hydraulic dust control). The fundamental work by V. P. Zhuravlev [29], A. A. Tsytsura [212], I. G. Ishchuk [213], and their students explains the mechanism of dust particulate and dispersed liquid interaction, discloses the optimum operating conditions, and offers design solutions for various sprinkling devices intended for bulk material transfer groups. This method became commonly used in mining and in the reprocessing of mineral raw materials. Hydraulic dust control is successfully used at ore preparation plants, at crushing and dressing plants, and with iron ore conveyer systems. However, the hydraulic dust control method was not commonly used in heat treatment of bulk materials at sintering plants because of additional energy consumption (for drying of watered material) and deterioration of production quality due to thermal breakdown of pellets and agglomerate in drip irrigation. That is why, in addition to techniques used for forming an indiscrete mass of the transferred material, the plants utilize dry methods for reduction of dust content in the exhaust air, such as pre-treatment of air in the direction of its flow from the chute outlet to the suction air conduit system inlet. This method is widely used for developing various dust-collecting elements for hoods and dust-collection bags (see Chapter 5).

The dry method of dust emission control (suction) is more universally popular and, as seen in Table 1.1, is more effective for air containment and dedusting. Therefore, of the three trends in dust emission control, the second is the most

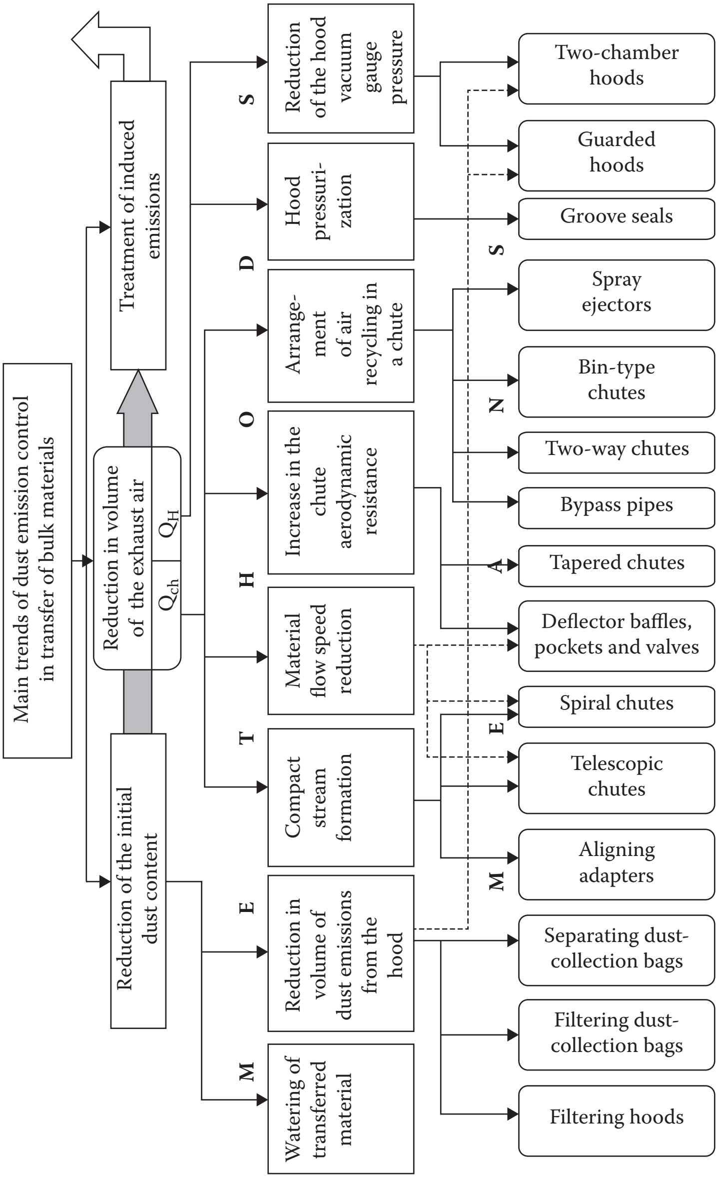

FIGURE 1.5 Primary methods and means of dust emission control in the transfer of bulk materials.

significant: reducing the induced air volume by controlling the air ventilation processes and sealing the hoods. By minimizing the output of suction hoods, it is possible to decrease the suction emission volume and significantly reduce the power consumption of ventilation units.

In order to implement effective control of the air suction process, it is necessary to understand the mechanism of intercomponent interaction and the regulation of the particle stream within the directed air, as well as taking into account the peculiarities of the enclosing walls' location (Figure 1.6). The geometric parameters of the bombarding particle stream are influenced by the consumption (G_M), initial velocity (υ_{init}), fineness (d), humidity (w), and self-adhesion properties of the material particles (σ_{self}). Stream behavior and structure are defined by bombarding particle velocity (υ), cross-sectional area (R), and particle distribution (β).

This dynamic interaction is subject to individual peculiarities of the aerodynamic resistance of bombarding particles (ARBP), such as the unit particle resistance coefficient (ψ_0), and to the common traits of the ARBP in the material stream—known as the reduced particle resistance coefficient (ψ^*) (see Chapter 2). When transferring hot materials, air suction is also influenced by the intensity of intercomponent heat exchange (see Chapter 3). The distance of non-permeable walls from the flow axis (r_0) creates various air leakage conditions and facilitates or complicates the suction process. When there is no such enclosure ($r_0 \rightarrow \infty$), the air suction is represented by a free flow of particles. In this case, an accelerated flow stream of induced air occurs in the stream (see Chapter 4). As the material stream nears the enclosure walls, air

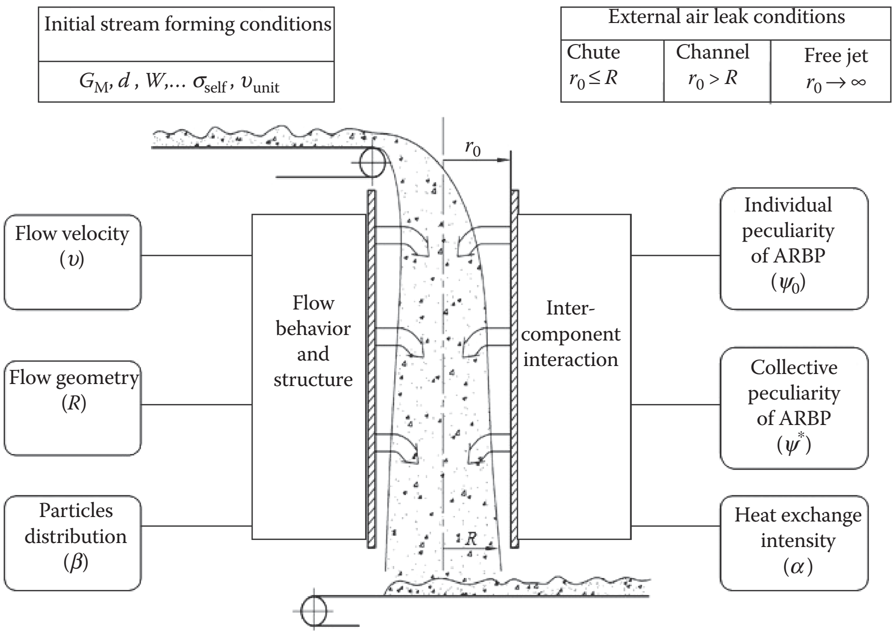

FIGURE 1.6 Qualitative structure and key factors that define the process of air suction with a bombarding particle stream.

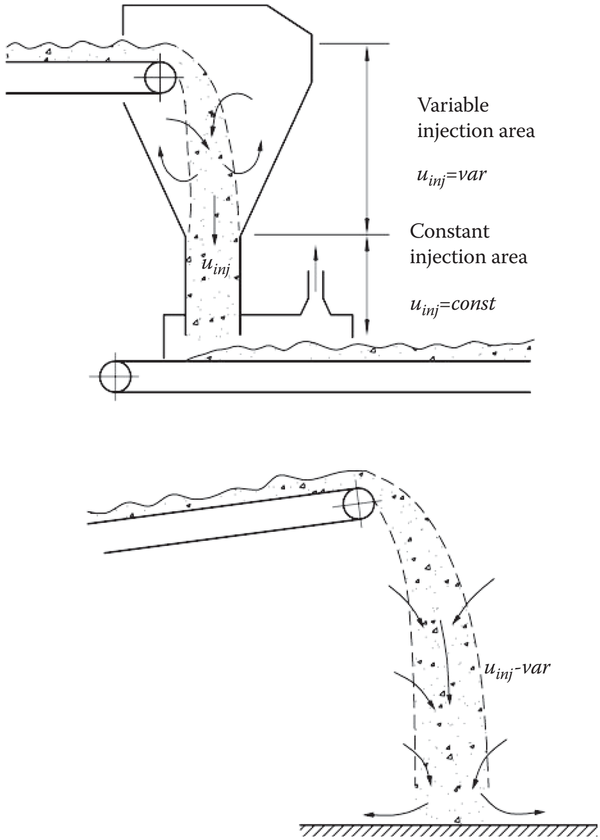

FIGURE 1.7 Typical bulk material transfer schemes (the upper scheme illustrates chute transfer; the lower scheme illustrates the free sedimentation).

leakage conditions deteriorate; an upward air stream (circulating stream) and/or a downward stream may occur. When $r_0 < R$ particles are falling down, the induced air formed in the section chute moves uniformly.

When pouring particles from the above-stack gallery (Figure 1.7), a free jet may be observed. In general, the most common chute transfer has combined leakage conditions. The most favorable air leakage conditions form at the receiving funnel inlet. First, the induced air jet is formed (accelerated suction area), then a uniform flow of induced air occurs (constant suction area), where particles enter into the straight portion of the small section chute ($r_0 < R$). This correlation between areas may be different in practice, however. In a receiving funnel, the chute height usually is much greater than the drop height, which impacts suction at the particle inlet stream.*

In bunker-type chutes, where the initial portion is much greater than the height of straight portions, transfers occur regularly—such as in chutes adjacent to sieves

* Nearly all design method guidelines skip the accelerated suction area except for OST 14-17-98-83 [73].

or to the discharge part of cone crushers. Typically, this is the case when the suction process is incorrectly considered to be constant within the channel of a phantom section (equal to the particle stream section or the bin outlet section).

The study of solid stream suction properties has a long history detailing suction process factors, the complex mechanism of particle motion, and the interaction between particles and air (Table 1.2) Experimental evaluation of suction properties in individual occurrences moved on to the development of mathematical models. These ranged from the simplest, such as an energy theory for uniformly accelerated stream of equidimensional particles in a vertical chute of uniform cross-section, to more complex models based on classical equations of multicomponent stream mechanics (see Appendix).

The large-scale implementation of sintering processes and the pelletizing of iron ore concentrates set a new challenge for the researchers—to determine the suction properties of a hot particle stream. This meant replacing the energy theory model with a more dynamic approach that treats air movement in a chute that is the result of forces that we call induction and thermal heads. Induction is the aerodynamic force of particles present in a chute. Thermal heads account for buoyancy forces that affect the air heated in the chute as a result of intercomponent heat exchange. This new theory enabled us to solve the problem of air suction and heated particles and to explain certain experimental facts, such as why reverse air flow (or anti-suction) occurs in a chute when unheated sand is poured into it (A. S. Serenko [85]). This new theory also explains the pressure surges that result when bulk material begins to fill (or stops filling) a pressurized vessel with a bulk material (see Chapter 2).

This theory explains the air suction process for a stream of bombarding particles and a complex process of air stratification (circulation) in a channel when a cross-section is partially occupied with bombarding particles (see Section 4.2).

1.2 THEORETICAL MODELS OF AIR SUCTION WITH A GRAVITATIONAL SOLID STREAM

When looking at the history of dust control method (suction) development from the quantitative (scientific) rather than the qualitative (structural) viewpoint, two periods of study should be considered.

The first period (1941–1949) is marked by experimental study of the suction process as a technical means of dust emission source containment. The most well-known studies are those conducted by Altmark, Rekk, Stakhorskiy, and Naumov in the Soviet Union and by Pring in the United States. These studies focused primarily on the problem of quantitatively assessing the phenomenon of air injection into a bulk material stream.

The second period of study, focusing on air injection research, may, in turn, be divided into two stages. The first stage involves suction property assessment in terms of energy. The fundamental efforts in this field were a study by S. E. Butakov (1949) of uniformly accelerated and distributed particle streams in a chute and the experimental study injecting air into a stream of water drops that was conducted in Utah by Pring, Knudsen and Dennis (1949). This field of study was further advanced in

TABLE 1.2
Studies of Solid Stream Suction Properties

Effects, Regularities	Methods, Notions	Authors
	Experimental Estimates	
Air movement in a vertical pipe when pouring sand (suction).	Inclined velocity of particles considered $u_{inj} = 0,48v_k$.	M. K. Altmark 1941
Reverse air flow when sand is moving in a chute.	Velocity and flow rate of particles as well as the chute cross-section considered.	A. S. Serenko 1953 [85]
	The same.	M. T. Kamyshenko 1955 [37]
	The same.	A. V. Sheleketin 1959 [102]
	All key factors considered.	E. N. Boshnyakov 1965 [11]
	The same.	Degner and Futterer 1969 [107]
	Mathematical Models	
A. Energy theory (based on the equation of the law of variation of kinetic energy of a stream of particles)		
	Subject to the analysis of the variation of kinetic energy of the uniformly accelerated stream of particles, there was an analytical relation obtained with the aim of determining the induced air flow rate.	S. E. Butakov 1949 [15]
	The same, the induction ratio notion was introduced.	O. D. Neykov 1965 [66]
Reduction in volume of the induced air with increase in the material flow rate.	The same as for powder material, "particle packet" and "nominal diameter" notions were introduced.	V. A. Minko 1969 [60]
B. Dynamic theory (based on the equation of variation of momentum of "solid particles-air" double speed continuum)		
Inhibiting effect on the volume of induced air of a stream of particles at the chute inlet. Reverse air flow in a chute when transferring particles at a high temperature (induction inversion).	There was the dynamic equation of the uniform air flow in a chute accounting of bulk forces of the dynamic and thermal interaction of components. The induction head notion was introduced.	I. N. Logachev 1969 [49]
Pressure surge when starting and ending to fill a sealed bin with bulk material.	There was an experimental method of determining the aerodynamic resistance of a group of bombarding particles in a chute (pressure measuring method).	1969 [52]
	Analytic studies of transient processes for an unsteady heated solid stream.	1974 [68]

continued

TABLE 1.2 (Continued)
Studies of Solid Stream Suction Properties

Effects, Regularities	Methods, Notions	Authors
	Analytic studies of the boundary-layer equation for a jet of air induced by a stream of bombarding particles.	1981 [69]
	There was a possibility of air circulation in a chute analytically demonstrated when the chute was partially filled with bombarding particles.	1987 [42]

the Soviet Union by O. D. Neykov (1965), E. N. Boshnyakov (1965), and V. A. Minko (1969), and in the United States by Hatch (1954), Hemeon (1955), Anderson (1964), and Cruise and Bianconi (1966). The second stage will be discussed in Section 1.2.3 of this chapter.

1.2.1 Butakov–Hemeon Model and Its Development

The Butakov–Hemeon model was built on the assumption that part of the momentum energy of a stream of particles E_1 is lost when surmounting environmental resistance. These losses are determined through the material particles' air drag R_0:

$$dE_1 = N_k \cdot R_0 \cdot dx = N_k \cdot R_0 \cdot v_1 \cdot d\tau, \tag{1.1}$$

where N_k is the number of bombarding particles per second. This energy is transmitted to the air, thereby moving it in order to surmount the chute drag.

The quantity of air energy (power) E_2 can be expressed through air flow rate and drag as

$$dE_2 = L_E dp. \tag{1.2}$$

If dE_1 and dE_2 are equal, the integration results in the following:

$$L_E \cdot p = \int_0^l N_k \cdot R_0 \cdot dx \cdot \tag{1.3}$$

It should be noted that some degree of inaccuracy is assumed in this case. When comparing Equations 1.1 and 1.2, it is assumed that the lost energy of bombarding particles is fully applied to the translational motion of air in a chute. However, only a portion of the lost energy is actually applied to accomplish this "useful" work while the rest of the energy goes to "mix" the induced air with a penetrating stream of particles. Introducing the energy transfer coefficient η_T to account for the portion of the bombarding particles' energy that is consumed to create a directional air flow, we obtain a more accurate result:

$$L_E \cdot p = \eta_T \cdot \int_0^l N_k \cdot R_0 \cdot dx. \tag{1.4}$$

The pressure difference is expressed by the sum of local drag factors:

$$p = \sum \zeta \cdot \frac{v_2^2}{2} \cdot \rho_2. \tag{1.5}$$

Then

$$R_{ch} \cdot L_E^3 = \eta_T \cdot \int_0^l N_k \cdot R_0 \cdot dx, \tag{1.6a}$$

where

$$R_{ch} = \sum \zeta \cdot \frac{\rho_2}{2 \cdot S_{ch}^2}. \tag{1.6b}$$

Expanding the integral value on the right side of Equation 1.6 with

$$R_0 = \psi_0 \cdot \frac{\pi \cdot d^2}{4} \cdot \frac{(v_1 - v_2)^2}{2} \cdot \rho_2, \tag{1.7}$$

$$v_1 = \sqrt{2 \cdot g \cdot x}, \tag{1.8}$$

for $\eta_T = 1$, S. E. Butakov obtained [15] the following:

$$Q^3 + a \cdot Q^2 + b \cdot Q + c = 0, \tag{1.9}$$

where $a = -A \cdot h/K \cdot F^2$, $b = 0{,}6 \cdot A \cdot h^{1,5}/K \cdot F$, $c = -A \cdot h^2/K$,

$$A = n \cdot k \cdot \frac{\pi \cdot d^2}{4} \cdot \frac{\gamma_b}{2} = 0{,}392 \cdot n \cdot k \cdot \gamma_b \cdot d^2,$$

$$K = \sum \zeta \cdot \frac{\gamma_b}{2 \cdot g \cdot F^2}, \quad n = \frac{6 \cdot G_M}{\pi \cdot d^3 \cdot \gamma_M};$$

where h = material drop height, m; K = chute hydraulic characteristic; F = chute cross-sectional area, m^2; γ_b = specific air weight, kG/m^3; d = diameter of particles, m; k = head drag coefficient of particles; n = number of particles per 1 sec; G_M = material weight flow rate, kG/s; γ_M = specific material weight, kG/m^3; and Q = induced air flow rate, m^3/s. Therefore, Equation 1.9 may be rewritten as:

$$\frac{\varphi^3}{6 \cdot \varphi^2 - 8 \cdot \varphi + 3} = \frac{Bu}{12}, \tag{1.10}$$

where the number

$$Bu = \frac{2 \cdot G_1 \cdot v_{1k}}{\Sigma\zeta \cdot c^2 \cdot \rho \cdot S_{ch}} \tag{1.11}$$

is hereinafter referred to as the Butakov–Neykov criterion (an inverse value of a modified Euler criterion)

$$Bu \equiv 1/Eu_m. \tag{1.12}$$

The initial equation (1.9) was first reduced to a dimensionless equation (1.10) by O. D. Neykov [66], who had analyzed the quantitative results of S. E. Butakov's model. In particular, multiple values were noted with respect to functions $\varphi = f(Bu)$ in the range $8.7 < Bu < 13.92$. It is therefore assumed that only the ranges $0 < \varphi < 0.807$ corresponds to the physics of the phenomenon in question and resultsing in the acceptance of $\varphi = 0.807$ and $Bu > 13.92$ without further proof.

It is important to bear in mind that Equation 1.7 does not account for the reversed direction of particle drag force at different levels in a chute (the second inaccuracy found in S. E. Butakov's model). A more accurate form of this force is represented as follows:

$$R = \psi \cdot f_M \cdot \frac{|v_1 - v_2| \cdot (v_1 - v_2)}{2} \cdot \rho_2. \tag{1.13}$$

At the chute inlet, the induced air speed may exceed the material movement speed when the latter is at its maximum, drag force $R < 0$ (i.e., particles at the chute inlet may cause additional flow resistance to the air suction).

Because of this, Equation 1.10 yields a slightly conservative value for induced air volumes.

Considering this same phenomenon, N. F. Grashchenkov, V. S. Kharkovskiy, and B. Tsoy developed the following formula for the induced air quantity [27]:

$$Q = 0{,}63 \cdot k \cdot \sqrt[3]{c \cdot \rho \cdot G \cdot t \cdot (\omega_k^3 - \omega_0^3) / (R \cdot d)}, \tag{1.14}$$

where G is material flow rate, m^3/s; ρ is air density, kg/m^3; c is a head drag coefficient; d is an equivalent sphere diameter, m; R is an aerodynamic drag of the chute, $kg \cdot s^2/m^8$; k is a correction factor (k = 0,18 for vertical chutes); ω_0, ω_k are relative velocities of material particles at the chute inlet and outlet, respectively, m/s; and t is a time period during which particles are in a chute, s.

Considering Equation 1.8, Equation 1.14 can be easily reduced to the following form:

$$\frac{\varphi^3}{(1-\varphi)^3 + \varphi^3} = \frac{k^3}{3}.Bu. \tag{1.15}$$

Looking at S. E. Butakov's model for a situation where drag force is proportional to relative velocity squared and is in a different direction based on the relative velocity sign, P. Ch. Chulakov, N. N. Korabekov, and K. S. Salimzhanov [101] obtained:

$$\frac{K}{N}=\frac{\lambda^3}{6\cdot\lambda^2-2\cdot\lambda^4-8\cdot\lambda+3}, \tag{1.16}$$

where

$$\frac{K}{N}=\frac{G\cdot c\cdot\rho\cdot h}{8\cdot v_k\cdot d\cdot\gamma_M\cdot R\cdot F_T^3},\ \lambda=\frac{v_2}{v_k}; \tag{1.17}$$

G is the material weight flow rate, N/s; γ_M is the material specific weight, N/m^3; d is a mean equivalent diameter of pieces, m; c is a head drag coefficient; h is a chute height, m; F_T is a chute cross-sectional area, m^2; v_k is the bounded bombarding velocity of particles, m/s; R is an aerodynamic drag of the chute, N·s^2/m^8; and ρ is air density, kg/m^3.

Using these symbols, Equation 1.16 will appear as:

$$\frac{\varphi^3}{6\cdot\varphi^2-2\cdot\varphi^4-8\cdot\varphi+3}=\frac{\mathrm{Bu}}{12} \tag{1.18}$$

When integrating dynamic equations for a particle and converting Equation 1.3, V. A. Minko [60] assumed that

$$\psi = 4{,}1\cdot\chi\cdot\mathrm{Re}^{-0{,}3}. \tag{1.19}$$

To obtain the following design ratio for particles of 0,2 mm < d < 2,5 mm and $v_1 < c$:

$$\frac{\lambda^3}{1-2{,}28\lambda+1{,}28\lambda^2}=2{,}8\cdot10^{-2}\cdot\frac{H\cdot v_1^{0{,}7}}{d^{1{,}3}}, \tag{1.20}$$

where

$$H=\frac{0{,}135\cdot\chi\cdot G}{\rho_M\cdot R\cdot F^3},$$

$$R=\sum\zeta\cdot\frac{\rho_b}{2\cdot F^2}, \tag{1.21}$$

and λ is the relation of the induced air speed to the material particles' bombarding speed; v_1 is the particles' bombarding speed in a stationary phase, m/s; G is the material flow rate, kg/s; ρ_M is the material density, kg/m^3; χ is an impact factor of particle shape; F is a chute cross-sectional area, m^2; $\Sigma\zeta$ is a sum of local drag factors for a chute; ρ_b is air density, kg/m^3; and d is a diameter of particles, m.

Inserting these symbols into Equation 1.20, we obtain:

$$\frac{\varphi^3}{1-2{,}28\cdot\varphi+1{,}28\cdot\varphi^2}=\frac{\mathrm{Bu}}{3{,}7}, \tag{1.22}$$

where

$$\mathrm{Bu} = \frac{\psi \cdot k_m \cdot G_1 \cdot v_{1k}}{g \cdot \rho_1 \cdot S_{ch} \cdot \Sigma\zeta}, \quad (1.23)$$

and ψ is the coefficient determined from Equation 1.19.

O. A. Bogaevskiy and U. H. Bakirov [8] considered a stream of particles with the initial velocity $v_{1\mathrm{H}}$ and the acceleration equal to:

$$a_m = 0{,}5(g+a_k), \quad (1.24)$$

where a_k is a particle's acceleration at the end of its fall in still air, m/s^2. They assumed that the process of air induction with such a particle stream is similar to S. E. Butakov's model and obtained:

$$Q = 3\varepsilon G \cdot h\rho/(8 \cdot \gamma_{\mathrm{M}} \cdot r), \quad (1.25)$$

where Q is the induced air volume, m^3/s; G is the material weight flow rate, kg/s; γ_{M} is the specific weight of material particles, kg/m^3; r is a radius of particles, m; h is a drop height, m; ε is an aerodynamic drag factor; and ρ is a correction factor (for iron ore of normal humidity $\rho = 0{,}3$).

Converting to these symbols, we obtain:

$$L_E = 6 \cdot \psi \cdot G_1 \cdot v_k^2 \cdot \rho_2 / (16 \cdot g \cdot \rho_1 \cdot d) \quad (1.26)$$

or

$$\varphi_k = \frac{1}{4} \rho \cdot \mathrm{Bu} \cdot \Sigma\zeta. \quad (1.27)$$

P. I. Kilin [39,40], having replaced the integral of the right side of Equation 1.3 with the sum of averaged values, studied S. E. Butakov's model with respect to chutes with a random number of straight sections. In particular, he suggested the following equation for a chute with a straight section:

$$\lambda = (\sqrt{9 + N \cdot M} - 3) / M, \quad (1.28)$$

where

$$N = 3 + 2 \cdot \frac{k \cdot d}{c_x \cdot l} \cdot \frac{v_k^2 - v_H^2}{v_M^2}; \quad M = \frac{d}{c_x \cdot l} \cdot \frac{\Sigma\zeta_{ch}}{S} \cdot \frac{v_k + v_H}{v_M} - 3; \quad (1.29)$$

$$S = \frac{G_M}{F \cdot \rho_M \cdot v_M}; \quad v_M = \frac{2}{3} \cdot \frac{v_k^3 - v_H^3}{v_k^2 - v_H^2}; \quad (1.30)$$

v_H, v_k are material velocities at the chute inlet and outlet, m/s; $\lambda = v_{\mathrm{B}}/v_{\mathrm{M}}$; v_{B} is air velocity in a chute, m/s; G is the material flow rate, kg/s; F is a chute cross-sectional area, m^2; ρ_M is a density of material particles, kg/m^3; c_x is a head drag coefficient; d is the mean diameter of material particles, m; l is a chute length, m; $\sum\zeta_{ch}$ is a sum of local drag factors of a chute; and k is a factor of apparent mass (assumed to be equal to 0,5).

For a vertical chute with $v_{1H} = 0$, $N \approx 3$, Equation 1.28 becomes:

$$\varphi_k = \frac{3}{2} \cdot \frac{\sqrt{Eu_m} - 1}{Eu_m - 1}. \tag{1.31}$$

V. A. Popov [77,78] theoretically analyzed S. E. Butakov's model for a bulk material considering the impact of environmental resistance on falling velocity. Assuming that iron ore concentrate and apatite move as a stream of blocks (10–60 mm in size with the conveyer belt width reaching 1000 mm), he proposed the following equation for induced air velocity (v_B) when transferring these materials:

$$v_B^3 - \frac{K \cdot h}{N} \cdot v_B^2 + 2 \cdot A \cdot \frac{K}{N} \cdot v_B - B \cdot \frac{K}{N} = 0, \tag{1.32}$$

where

$$K = ncf\rho; \quad N = 2RF^3; \tag{1.33}$$

h is a material drop height; A and B are coefficients accounting for variations in the velocity of blocks of material particles that are due to environmental resistance; n is the number of blocks per 1 sec; $c = 1.15$ is a drag coefficient of blocks; f is a block cross-sectional area; ρ is air density; R is a chute hydraulic characteristic; and F is a chute cross-sectional area.

Incorporating these factors, Equation 1.32 will appear as:

$$\frac{\varphi_k^3}{6 \cdot \varphi_k^2 - 8 \cdot k_1 \cdot \varphi_k + 3 \cdot k_2} = \frac{\mathrm{Bu}}{12}, \tag{1.34}$$

where

$$k_1 = \frac{1{,}5 \cdot A}{h \cdot \sqrt{2 \cdot g \cdot h}}; \quad k_2 = \frac{B}{g \cdot h^2}. \tag{1.35}$$

To determine aerodynamic force (assuming still air), Hemeon solved Equation 1.3 as follows [109]:

$$L_E^3 \frac{\rho_2}{2S_{ch}^2} = \int_{v_{1H}}^{v_{1\kappa}} \bar{\beta}_1 l S_{ch} k_m \psi \frac{v_1^2}{2} \rho_2 dv_1, \tag{1.36}$$

where $\bar{\beta}_1$ is a bulk concentration averaged along the chute length

$$\bar{\beta}_1 = \frac{1}{l} \int_0^l \frac{G_1}{\rho_1 S_{ch} v_1} dx = \frac{2G_1}{\rho_1 S_{ch} (v_{1H} + v_{1\kappa})}, \tag{1.37}$$

$$\bar{\beta}_1 S_{ch} l = \frac{2lG_1}{\rho_1 (v_{1H} + v_\kappa)}. \tag{1.38}$$

(The last formula is simply a chute volume filled with material.)

Hemeon expanded the right-hand side of Equation 1.36 for three cases: (a) for the self-similarity area

$$\psi = \psi_0 \text{ at Re} > 500; \tag{1.39}$$

(b) for the transition area

$$\psi = \text{a/Re}^{0,6}; \tag{1.40}$$

and (c) for the airborne area when

$$v_1 = c - const.$$

In the latter case, the drag force in Equation 1.3 was replaced with the gravity force. Thus, the hydraulic resistance of the chute and the air motion within the chute were not considered. It was assumed that the count concentration (and, hence, the bulk concentration) is constant throughout the chute length.

For the self-similarity area ($\psi_0 = 0.44$) with $v_{1H} = 0$, $v_1 = \sqrt{2gh}$ Hemeon obtained:

$$Q = \sqrt[3]{7 \cdot \frac{R \cdot S^2}{\gamma_3 d} \cdot A^2 \cdot 1200}, \tag{1.41}$$

where Q is the induced air flow, m^3/s; S is the total drop height, m; R is the material flow rate, kg/s; A is a flow area of particles, m^2; γ_3 is the material density, kg/m^3; d is a diameter of particles, m; and h is the present bombarding height of particles, m.

Equation 1.41 will then appear as follows:

$$L_E = 20,3 \cdot \sqrt[3]{G_1 \cdot H^2 \cdot S_{ch} / (\rho_1 \cdot d)} \tag{1.42}$$

or

$$\frac{\varphi_k^3}{(1-n) \cdot (1-n^3)} = \frac{\Sigma\zeta}{3 \cdot Eu_m}. \tag{1.43}$$

Hatch [108], having noticed excessive results from Equation 1.41, introduced the efficiency factor:

$$Q = 0,78 \cdot \sqrt[3]{E \cdot T \cdot A^2 \cdot h^2 / (z \cdot d)}, \tag{1.44}$$

where Q is the induced air quantity, ft^3/min; T is the material flow rate, t/hr; h is a drop height, ft; A is a flow area of particles, ft^2; d is the mean mass diameter of particles, inches; z is the material density, g/cm^3; and E is the efficiency factor.

Equation 1.44 then becomes:

$$L_E = 17{,}4 \cdot \sqrt[3]{EG_1 H^2 S_{ch}^2 / (\rho_1 \cdot d)} \tag{1.45}$$

or

$$\frac{\varphi_k^3}{(1-n)\cdot(1-n^3)} = \frac{\Sigma\zeta \cdot E_E}{3 \cdot Eu_m}\,. \tag{1.46}$$

Morrison [112] introduced a correction factor into Hemeon's equation for transfers of polyfractional material:

$$Q = 110 \cdot \sqrt[3]{T \cdot H^2 \cdot A^2 / (G \cdot D)}\,, \tag{1.47}$$

where Q is the induced air quantity, ft^3/min; S is the material flow rate, t/hr; H is a drop height, ft; A is a flow area of particles, ft^2; G is the material density, pound/ft^3; and D is the mean diameter of material particles, inches. Therefore:

$$L_E = 6{,}3 \cdot \sqrt[3]{G_1 \cdot H^2 \cdot S_{ch}^2 / (\rho_1 \cdot d)}\,. \tag{1.48}$$

Considering the hydraulic resistance of chute walls to induced air movement, Anderson and Dennis [106] replaced the chute cross-section in Hemeon's equation with the upper hood leakage area to correspond with $F_b \le 0.15$B (where F_b is the upper hood leakage area, m^2; B is the feed conveyer belt width, m), resulting in:

$$Q_1 = 10 \cdot A_u \cdot \sqrt[3]{R \cdot S^2 / D}\,, \tag{1.49}$$

where Q_1 is the induced air quantity, ft^3/min; A_u is the upper hood leakage area, ft^2; R is the material flow rate, t/hr; S is a drop height, ft; and D is the mean diameter of particles, ft. Using symbols, this becomes:

$$L_E = 1{,}5 \cdot F_b \cdot \sqrt[3]{G_1 \cdot H^2 / d}\,,\ \text{m}^3/\text{s}. \tag{1.50}$$

Cruise and Bianconi [110] took the material flow area for an initial parameter and did not relate it to the chute cross-section (introduced in Hemeon's formula as the chute cross-sectional area):

$$F_{con} = k \cdot G_1 / (\rho_n \cdot v_1)\,, \tag{1.51}$$

where ρ_n is material mass in a stream volume unit determined by the empirical function:

$$\rho_n = 5{,}4 \cdot \rho_1 \cdot d^{\,0{,}3}; \tag{1.52}$$

ρ_1 is a density of particles, g/cm^3; d is a diameter of particles, inches; and k is a trial coefficient.

This data satisfactorily matched experimental data from studies of coal transfers with $S_{ch} = 0.56 \div 1.12$ m^2, $G_1 \geq 0.28$ kg/s, d ≥ 1.27 mm, $\rho_1 = 1300$ kg/m^3, and $H \sim 2$ m obtained with calculations according to the formula:

$$Q = 10{,}5 \cdot T \cdot \sqrt[3]{h} \cdot d^{-0{,}5} \cdot z^{-1} \cdot \exp(-6{,}5 \cdot k), \tag{1.53}$$

where Q is the induced air quantity, ft^3/min; T is the material quantity transferred, t/hr; h is a drop height, ft; d is the mean diameter of material, inches; z is the material density, g/cm^3; k is the efficiency factor equal to $k = N{\cdot}90/(h{\cdot}\theta)$; N is the number of chute revolutions; and θ is the chute inclination angle, deg. Using symbols:

$$L_E = 132 \cdot G_1 \cdot H^{1/3} \cdot d^{-0{,}5} \cdot \rho_1^{-1} \cdot \exp(-1{,}98 \cdot k). \tag{1.54}$$

1.2.2 Semiempirical Models

Now we will focus on some empirical formulas widely used to assess the injective capacity of a stream of bulk material.

Using a stream of crushed granite ($\rho_1 = 2630 \div 2660$ kg/m^3, d = 22.6 mm and 11.2 mm), M. T. Kamyshenko [37] obtained the following empirical equation (with $G_1 = 1.4 \div 18.1$ kg/s, H = 1.315; 1.755; 2.275 m in a vertical pipe of D = 260 mm):

$$Q_B = \frac{G_M}{1{,}2} \cdot \frac{F_T}{f_M} \cdot \mathrm{tg}\beta, \tag{1.55}$$

where

$$f_M = G_M / (\gamma_M \cdot v_{B\kappa} \cdot 3600);$$

Q_B is the induced air volume, m^3/hr; F_T is the chute cross-sectional area, m^2; G_M is the material flow rate, t/hr; f_M is the chute section area filled with falling material; γ_M is the material bulk weight, t/m^3; v_{BK} is the bombarding velocity of particles at the chute inlet assumed to be equal to the upper conveyer speed, m/s; and tgβ is slope ratio of linear dependence.

Having assumed that tgβ = $0.0038{\cdot}v_K^2$, A. M. Gervasiev [21] converted Kamyshenko's equation ($F_B/S_{ch} \leq 0.3$) to determine induced air quantity (Q_E) by using the following formula:

$$Q_E = 0{,}04 \cdot k_y \cdot Q_M \cdot v_\kappa^2, \tag{1.56}$$

where Q_M is the material volume flow rate, m^3/hr; k_y is hood structure-dependent factor ($k_y = 1.35 \div 3.0$); and v_K is the material flow rate at the chute outlet, m/s.

For transfers of quartzite particles (with a fineness of $0.5 \div 1$ mm and $3 \div 5$ mm with F_{ch} = 0.075; 0.06; 0.035 m^2; H = 1, 2, 3 m; Θ = 45, 50, 70 deg.), A. V. Shelektin [102] found:

$$Q_{ch} = 1{,}16 \cdot k \cdot G_M^{0{,}2} \cdot F_{ch}^{0{,}8}, \tag{1.57}$$

where Q_{ch} is the induced air volume, m^3/hr; G_M is the material quantity transferred, kg/hr; F_{ch} is the chute cross-sectional area, m^2; and k is a factor accounting for a drop height H and the chute inclination Θ.

For coal transfers (in $2.5 < v_K < 11.5$ m/s; $5 < Q_y < 170$ dm^3/s; $0.14 < F_{ch} < 1.25$ m^2; $40° < \Theta < 90°$), A. P. Lyubimova [56] found:

$$Q_E = \frac{0,29 \cdot k_\alpha \cdot v_k \cdot Q_y^{0,3} \cdot F_{ch}^{0,7}}{d^{0,34 \cdot \varphi} \cdot c_H^{0,87}}, \tag{1.58}$$

where Q_E is the induced air volume flow rate, m^3/s; Q_y is coal volume flow rate, m^3/s; v_K is a bounded coal falling velocity, m/s; F_{ch} is the chute cross-sectional area, m^2; d is the particle diameter, m; k_α, φ are factors accounting for the influence of nonuniformity of an in-depth distribution of a solid ingredient feed concentration and the quantity of a surface of an active interaction of particles with air based on the chute inclination; and c_H is the relation of the chute cross-sectional area to the leakage area.

Having analyzed the air induction with a stream of steel spheres, V. D. Olifer [71] obtained the design ratios for the dynamic interaction force:

$$P_E = \rho \cdot (\bar{v}_M - \bar{v}_B)^2 \cdot \left(\frac{h}{h_{e\partial}}\right)^{1,75} \cdot \bar{k}^{1,25} \cdot \left[0,81 + \frac{1,68 \cdot 10^6 \cdot \nu^2}{(\bar{v}_M - \bar{v}_B)^2 \cdot d_{av}^2}\right] \tag{1.59}$$

as well as for velocity of the induced air in a chute for transfers of spherical particles and irregularly shaped particles:

$$\bar{v}_B^2 \cdot \left(\frac{\zeta_n}{1,265} - 1\right) + 2 \cdot \bar{v}_M \bar{v}_B - \bar{v}_M^2 - \frac{482}{d_{av}^2} - 1,32 \cdot \frac{P}{S} = 0, \tag{1.60}$$

where $\bar{v}_B$ is an average air velocity in a chute, m/s; $\bar{v}_M = 0,7 v_M^H + 0,3 v_M^\kappa$ is an average material velocity in a chute, m/s; v_M^H, v_M^K are material velocities at the chute inlet and outlet, respectively, m/s; d_{av} is the mean diameter of particles, mm; P is the lower hood vacuum-gauge pressure, Pa; and S is the sum total:

$$S = m \cdot N \cdot \bar{k} \cdot (h / h_{e\partial})^{1,5}, \tag{1.61}$$

where $m = 1.3 f_p - 0.3$; f_p is a particle geometric form factor; N is a coefficient (with $d_{av} > 3.5$ mm, $N = 1$); $\bar{k} = 100 \cdot W / (F_{ch} \cdot \bar{v}_M)$; W is the material volume flow rate, m^3/s; F_{ch} is the chute cross-sectional area, m^2; ζ_n is a sum of local drag factors of the chute and the upper hood; h is the chute height, m; and $h_{e\partial}$ is the chute unit height (equal to 3 m).

When $N = 1$, $v_{1H} = 0$, P = 0, $h = h_{e\partial} = 3$ m, Equation 1.60 may be rewritten as follows:

$$\varphi_k^2 \cdot \left[\frac{10,8}{d_{av}} \cdot Eu_m - 1\right] + 0,6 \cdot \varphi_k - 0,09 - \frac{8}{d_{av}^2} = 0, \tag{1.62}$$

where d_{av} is the mean diameter of particles, mm.

Following experimental studies, E. N. Boshnyakov [10,11] obtained this design ratio for induced air volume (Q_e):

$$Q_e = 3{,}165 \cdot k_H \cdot k_G \cdot k_{v0} \cdot k_F \cdot k_{\sum\zeta} \cdot k_c \cdot k_d \cdot k_\gamma \cdot k_h, \tag{1.63}$$

where k_H is the material transfer height (the material velocity at the chute outlet), k_G is the material flow rate, k_{v0} is the initial velocity, k_F is the chute cross-sectional area, $k_{\Sigma\zeta}$ are local drag factors, k_c is a head drag of the material particles, k_d is the fineness of particles, k_γ is the material density, and k_h is the hood vacuum-gauge pressure.

After reducing the experimental data, Degner and Futterer [107] obtained the following equation for transfers at coal preparation plants:

$$Q = \frac{k_1 \cdot M^\alpha \cdot F_{E0}^\beta \cdot (F_{su}^\nu + k_2) \cdot H^\delta \cdot v_B^\vartheta \cdot F_s}{d^\varepsilon \cdot \rho^\zeta \cdot z^\eta}, \tag{1.64}$$

where M is the material mass flow rate; F_{E0} is the leakage area in the chute receiver portion hood; F_{su} is the leakage area in the chute discharge outlet hood; F_s is the chute cross-sectional area; H is a material transfer height; v_B is the feed conveyer belt speed; d is the mean diameter of material grains; ρ is the material density; z is the number of seal covers; and k_1, k_2, α, β, ν, δ, ϑ, ε, ζ, and η are trial coefficients.

After having analyzed the air mechanics of a stream of steel spheres, particles of coal, millet, peas, rice, wheat, and lentils in a vertical pipe, V. P. Pavlov [74] obtained the following empirical equation (with $D_0/d_e = 9 \div 27$; $l/d_e = 75 \div 614$; and $v_f/v_{Bum} = 0 \div 1.34$) for the air velocity along the material stream axis (v_f^0):

$$v_f^0 / v_{Bum} = 0{,}0174 \cdot \left(l/d_e \right)^{0{,}51} \cdot \left(v_f / v_{Bum} + 1 \right)^{1{,}82} \cdot \left(D_0/d_e \right)^{-0{,}2}, \tag{1.65}$$

where v_f is the velocity of undisturbed air flow outside the jet; v_{Bum} is the airborne velocity of particles; l is the jet length; D_0 is the initial diameter of a jet; and d_e is a diameter of a sphere equivalent to a particle in its volume.

Experimental studies by M. T. Kamyshenko (1951), A. S. Serenko (1953), and A. V. Sheleketin (1959) built empirical relations for determining L_E and for discovering new effects (reverse air flows and pressure surges in closed chutes) that had been unexplainable for a considerable time period.

1.2.3 Dynamic Theory and Research Methodology for Injection Properties of a Particle Stream

The second stage, the study of aerodynamic processes in a bulk material stream in terms of two-component flow dynamics, was initiated by one of the authors in 1964 at the Krivoy Rog branch of the Institute of Mining Affairs of the Academy of Sciences of the Ukrainian Soviet Socialist Republic (presently NIIBTG) following the solution of hot material transfer suction problems [36,51,52].